

Article

# Morphological Study and 3D Reconstruction of the Larva of the Ascidian *Halocynthia roretzi*

Lucia Manni <sup>1,\*</sup> , Federico Caicci <sup>1</sup> , Chiara Anselmi <sup>2,3</sup>, Virginia Vanni <sup>1</sup> , Silvia Mercurio <sup>4</sup>   
and Roberta Pennati <sup>4,\*</sup> 

<sup>1</sup> Department of Biology, University of Padova, 35131 Padova, Italy; federico.caicci@unipd.it (F.C.); virginia.vanni@phd.unipd.it (V.V.)

<sup>2</sup> Department of Biology, Hopkins Marine Station, Stanford University, Pacific Grove, CA 93950, USA; chiara90@stanford.edu

<sup>3</sup> Institute for Stem Cell Biology and Regenerative Medicine, Stanford University School of Medicine, Stanford, CA 94305, USA

<sup>4</sup> Department of Environmental Science and Policy, University of Milano, 20133 Milano, Italy; silvia.mercurio@unimi.it

\* Correspondence: lucia.manni@unipd.it (L.M.); roberta.pennati@unimi.it (R.P.)

**Abstract:** The swimming larva represents the dispersal phase of ascidians, marine invertebrates belonging to tunicates. Due to its adhesive papillae, the larva searches the substrate, adheres to it, and undergoes metamorphosis, thereby becoming a sessile filter feeding animal. The larva anatomy has been described in detail in a few species, revealing a different degree of adult structure differentiation, called adulation. In the solitary ascidian *Halocynthia roretzi*, a species reared for commercial purposes, embryogenesis has been described in detail, but information on the larval anatomy is still lacking. Here, we describe it using a comparative approach, utilizing 3D reconstruction, as well as histological/TEM observations, with attention to its papillae. The larva is comparable to those of other solitary ascidians, such as *Ciona intestinalis*. However, it displays a higher level of adulation for the presence of the atrium, opened outside by means of the atrial siphon, and the peribranchial chambers. It does not reach the level of complexity of the larva of *Botryllus schlosseri*, a phylogenetically close colonial ascidian. Our study reveals that the papillae of *H. roretzi*, previously described as simple and conform, exhibit dynamic changes during settlement. This opens up new considerations on papillae morphology and evolution and deserves to be further investigated.

**Keywords:** adhesive papillae; adulation; *Botryllus schlosseri*; *Ciona intestinalis*; tunicates



**Citation:** Manni, L.; Caicci, F.; Anselmi, C.; Vanni, V.; Mercurio, S.; Pennati, R. Morphological Study and 3D Reconstruction of the Larva of the Ascidian *Halocynthia roretzi*. *J. Mar. Sci. Eng.* **2022**, *10*, 11. <https://doi.org/10.3390/jmse10010011>

Academic Editor: Nick Aldred

Received: 30 November 2021

Accepted: 20 December 2021

Published: 24 December 2021

**Publisher's Note:** MDPI stays neutral with regard to jurisdictional claims in published maps and institutional affiliations.



**Copyright:** © 2021 by the authors. Licensee MDPI, Basel, Switzerland. This article is an open access article distributed under the terms and conditions of the Creative Commons Attribution (CC BY) license (<https://creativecommons.org/licenses/by/4.0/>).

## 1. Introduction

Ascidians are sessile marine invertebrates belonging to the tunicates, a group that is evolutionarily close to vertebrates [1]. Some species are gregarious and form complex clusters of several organisms living in close proximity [2]. They can colonize different natural and artificial substrates and can modify the primary substrate providing habitats for other organisms. Thus, ascidians are considered essential members of the benthic communities contributing to increased ecosystem complexity and biodiversity [3] and have been proposed as valuable model organisms to test coastal water pollution [4–6]. Ascidians also have economic importance since some species, such as *Halocynthia roretzi*, are commercially reared for human consumption [7,8]. For this reason, *H. roretzi* is one of the most studied ascidians: its genome is compact with about 16,000 protein-coding genes [9] and its development is known in detail [10]. Other species (such as *Ciona intestinalis*) are potential food and biofuel sources [4]. Some ascidians (such as *Botryllus schlosseri* and *Botrylloides violaceus*) are considered invasive organisms in marinas and also fouling organisms in marine aquaculture, and their presence results in economic loss [11].

Ascidians show an extraordinary range of life history traits, with some species being solitary and others showing colonial organisation; the latter evolved several times during

the diversification of the group [12,13]. Tunicate taxonomy has long been questioned; the group comprises approximately 3000 species that have traditionally been divided into three classes: Ascidiacea (sea squirts), Thaliacea (pelagic salps, doliolids and pyrosomes), and Appendicularia (larvaceans) [14]. Molecular based phylogenies revealed that Ascidiacea was paraphyletic [15,16] and the following three clades were proposed: (1) Stolidobranchia, (2) Appendicularia, and (3) Phlebobranchia plus Aplousobranchia plus Thaliacea [17].

Sessile adults develop from swimming lecithotrophic larvae that represent the dispersal stage of their life cycle. Larvae of different species show the same general body organisation corresponding to the basal body plan of chordates. The larva is formed by a trunk and a muscular tail used for locomotion. The trunk contains the anterior nervous system equipped with two pigmented sensory organs (the ocellus and otolith), mesenchyme cells and the endodermal pharynx, whereas the tail houses the notochord, the posterior neural tube dorsal to the notochord and lateral bands of muscle cells.

The larva is sheltered by the epidermis, which secretes the larval tunic, the characteristic external fibrous matrix of the phylum. The larval tunic exhibits two layers (compartments). The outer layer covers the trunk and the tail, forming, on the latter, continuous fins for swimming; this layer is lost at larval metamorphoses. The inner layer, called the definitive tunic, covers the trunk and is maintained during metamorphosis to constitute the tunic covering the adult body. Two cuticular layers thicken the layer surfaces [18–21].

Despite the gross anatomical similarities, ascidian larvae have been remodelled in different ways during evolution [22]. Colonial species, which produce yolked eggs, are ovoviviparous (or even viviparous) [23,24] and exhibit prolonged embryogenesis. Their larvae often undergo adulation, a mode of development in which adult structures differentiate precociously in the tadpole trunk. Adulation can manifest to different degrees, from the early appearance of siphons, a partial digestive tract, a few gill slits, a rudimentary heart, or one or more buds prior to asexual reproduction, up to involving more extensive development of adult structures [22,25]. For example, the larva of the colonial *Botryllus schlosseri* exhibits both open siphons, five pairs of perforated stigmata, a hollow heart, the rudiment of the adult nervous system close to the larval one, and two buds [26]. Caudalisation is another alternative mode of development present in ascidians consisting of the addition of muscle cells to the tadpole tail without changing the number of other larval cells. This enhances the swimming ability of the larva and its dispersal [22]. In comparison to colonial ascidians, solitary species, such as the model ascidian *Ciona intestinalis*, usually develop smaller eggs, are oviparous, and exhibit rapid embryogenesis producing relatively simpler larvae [21]. These reproductive and larval anatomical differences are surprising when exhibited by closely related species, such as the solitary *H. roretzi* and the colonial *B. schlosseri*, both of which are stolidobranch ascidians.

The larva plays a crucial role in ascidian life since it selects the substrate to adhere to permanently. Indeed, after hatching, the tadpole larva swims for up to a few days, then attaches to a substrate and undergoes metamorphosis: the tail is retracted into the trunk, the larval tissues are resorbed, and adult structures differentiate from rudiments in the trunk [27]. The critical step of substrate selection and adhesion is mediated by three mucus-secreting organs, the adhesive papillae (or palps) that most ascidian larvae bear at their anterior tip. Generally, the papillae are composed of elongated mucus-secreting cells, called colocytes (CCs), primary sensory neurons (PSNs) and supporting axial columnar cells (ACCs) [27]. It was proposed that papillary sensory cells are mechanosensory neurons playing a central role in substrate selection [28]. Actually, the morphology of adhesive papillae is quite variable among species, and they can be classified into 10 types according to their histological characteristics [27,29]. A major distinction can be traced between simple conic papillae that are present in most solitary ascidians, and the eversible papillae characteristic of some colonial species, which are capable of rapid eversion to expose sticky mucus. Due to their complexity and diversity, it is not surprising that larvae are of key importance for the taxonomic recognition of ascidian species. Indeed, ascidians are the only chordates identified also by larval characteristics [30,31].

In the model species *C. intestinalis*, the fine anatomy of the adhesive papillae has been extensively analysed. Each one of these organs are formed by exactly 20 cells: four ACCs surrounded by 12 CCs and flanked by two pairs of PSNs. The central ACCs, which have been suggested to have a chemosensory function, extend their apical endings into a hyaline cap. In *C. intestinalis*, they can be identified by the expression of the  $\beta\gamma$ -Crystallin gene [32]. CCs secrete the adhesive mucus responsible for performing the temporary adhesion to the substrate. PSNs are glutamatergic neurons that sense the substrate [33].

Although *H. roretzi* is a well-established model species in developmental biology, the overall morphology of the larva and the structure of its papillae have been poorly described. Therefore, in the present article, we present the first 3D reconstruction of the swimming larva of *H. roretzi* to gain insight into its morphology. We compare it with the 3D reconstruction of the close colonial species *B. schlosseri* and of the solitary species *C. intestinalis*, discussing the degree of adultation in the three models. Moreover, we focus on the description of the adhesive papillae of *H. roretzi* for their crucial role during larval settlement. Our data show that, despite the simple larval anatomy of *H. roretzi*, similar to that of other solitary ascidians, the papillae are dynamic structures that undergo retraction and remodelling during adhesion.

## 2. Materials and Methods

### 2.1. Animals

Adults of *Halocynthia roretzi* were collected near the Marine Biological Station “Asamushi” of the Tohoku University (Aomori, Japan). Embryos were obtained by in vitro fertilisation and were reared at 13 °C for 35 h until the larva hatched. Images of 47 larvae were taken using a Leica MZ16 Stereomicroscope and analysed by Photoshop software to determine the following morphometric parameters: total length of the larva, trunk length, tail length. The pool of larvae consisted of typical swimming larvae with protruded anterior papillae and larvae at the beginning of metamorphosis, with shorter papillae.

### 2.2. Histology

Larvae were fixed for 9 h in 1.5% glutaraldehyde in 0.2 M sodium cacodylate buffer at pH 7.2. at 4 °C. They were rinsed several times in 0.2 M sodium cacodylate and 1.7% NaCl buffer and then post-fixed for 1 1/2 h in 1% OsO<sub>4</sub> in 0.2 M cacodylate buffer at 4 °C. Samples were dehydrated and then soaked in Epon and propylene solution at 37 °C, 45 °C, and 60 °C. They were then embedded in epoxy resin (Sigma-Aldrich), oriented and sectioned using a Leica Ultramicrotome UC7. Five individuals at larval stage and three individuals at adhering larval stage were cut for histological analysis. Sections, 1 µm thick, were stained with toluidine blue in borax. Ultrathin sections (80 nm thick) were stained with uranyl acetate and lead citrate to provide contrast. Photomicrographs were taken with a FEI Tecnai G<sup>2</sup> electron microscope operating at 100 kV. Images were captured with a Veleta (Olympus Soft Imaging System) digital camera.

### 2.3. Three-Dimensional Reconstructions

A selected swimming larva of *H. roretzi* was embedded in resin as previously described and serially transversely cut using a Histo Jumbo Knife (Diatome). Sections, 1 µm thick, were arranged in chains of about 20 sections each and stained with toluidine blue. All the sections were then photographed with a Leica DMR optical microscope. Images were aligned using Adobe Photoshop CS on a Windows 10 computer. Based on the resulting stack of images, the 3D model of the anatomy of all organs but tunic was created in Amira software (ThermoFisher scientific, Waltham, MA, USA). For the comparison with the 3D reconstructions of larvae of *Ciona intestinalis* and *Botryllus schlosseri*, we used previously prepared datasets of serial sections [26,32].

### 3. Results

#### 3.1. The 3D Reconstruction of *Halocynthia roretzi* Larva

The *H. roretzi* larvae, 10 h post hatching at 12 °C, were found to be  $1744 \pm 18 \mu\text{m}$  long; the tail length is  $1252 \pm 15 \mu\text{m}$  and the trunk is  $490 \pm 6 \mu\text{m}$  (Figure 1, Table S1). At the anterior tip of the trunk, three adhesive papillae are arranged according to the vertices of an equilateral triangle (two dorsal, one ventral) (Figure 1A,B',G).

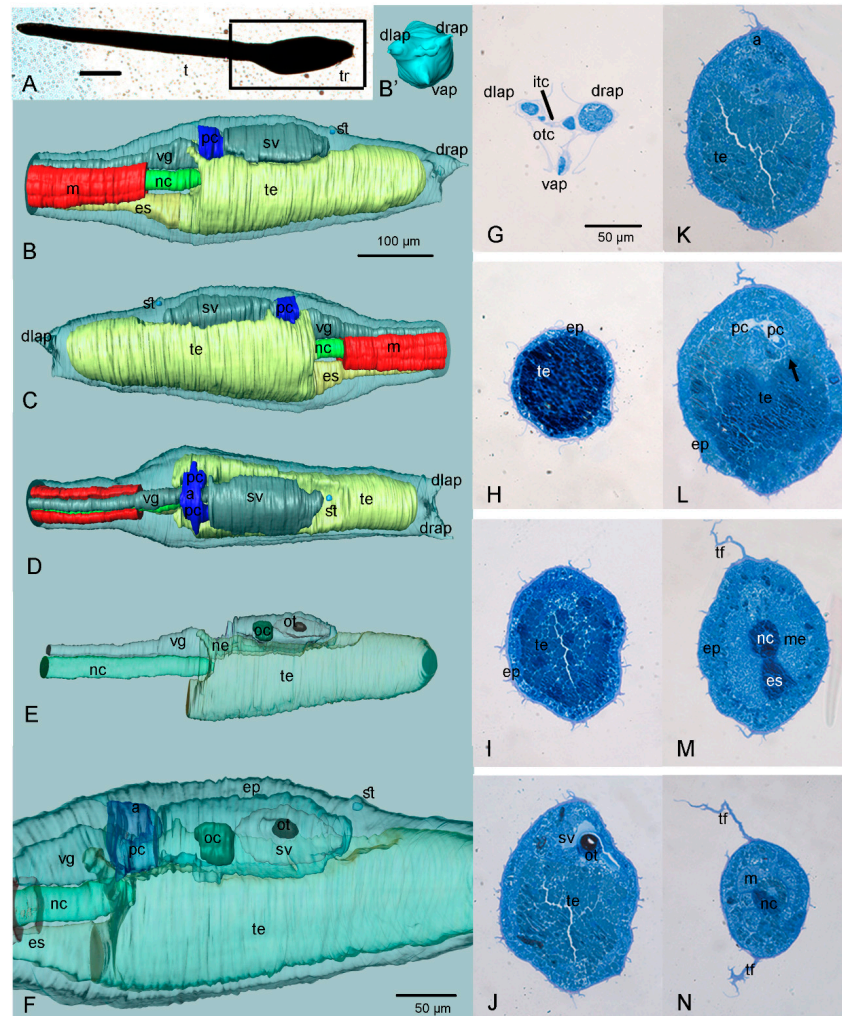


**Figure 1.** Anatomy of the larva of *H. roretzi* (see also the 3D-PDF of Figure S1; requires Acrobat Reader DC or higher). (A) Whole mount larva (in block of resin, contrasted with  $\text{OsO}_4$ ). Right side view. t: tail; tr: trunk. The black square indicates the trunk region illustrated in (B–E). (B–F) Three-dimensional reconstructions. Colour code: blue, atrial chamber; dark green, ocellus; grey, nervous system; light green, notochord; red, muscles; yellow, endoderm (i.e., prospective pharynx). In B–D, the epidermis is transparent; in (E,F), the organs are transparent and their internal structures can be seen. (B) Right side view. (B') Frontal view of the trunk showing the three papillae. (C) Left side view. (D) Dorsal view. (E) View of internal organs: trunk endoderm, nervous system and notochord. (F) Close view of the trunk region. (G–N) Some cross histological sections, from anterior to posterior, utilized for the 3D reconstruction. Toluidine blue. Arrow in L indicates the area where the protostigmata will open during metamorphosis. a: atrium; drap, dlap, vap: dorsal right-, dorsal left-, and ventral-adhesive papilla, respectively; ep: epidermis; es: endodermal strand; itc: inner tunic compartment; m: muscle; me: mesenchyme; nc: notochord; ne: neck; otc: outer tunic compartment; pc: peribranchial chambers; oc: ocellus; ot: otolith; st: stomodeum (i.e., oral siphon primordium); sv: sensory vesicle; te: trunk endoderm; tf: tail fin; vg, visceral ganglion. The enlargement is the same in (B–E) and in (G–N).

With respect to the histological sections, the 3D reconstruction allows a better understanding of the reciprocal positions of internal structures, the relative development of different organs and their anatomical details (Figure 1A–F; Figure S1; Video S1). Larval organs and tissues can be visualized in the MorphoNet browser at <https://morphonet.org/9vILe4SK>, accessed on 23 December 2021 [34]. The oral siphon primordium overlays the prospective pharynx that is differentiating from the trunk endoderm. The latter presents a narrow lumen (Figure 1I–K) and occupies most of the trunk, just under the nervous system (Figure 1B–D). The central nervous system is dorsal to the endoderm; in the trunk, it swells to form the sensory vesicle and, posterior to this, the visceral ganglion (Figure 1E–F). The two bulges are separated by a narrow neck as in other species, such as *Ciona intestinalis* (Figure 1E) [35]. The sensory vesicle is asymmetric and more enlarged on the right. It exhibits two pigmented sensory organs, the ocellus (occupying its posterior wall) and the otolith (emerging from its floor) (Figure 1F,J). The otolith is formed by a single large, pigmented cell (Figure 1J). A small, anteriorly blind, neurohypophyseal duct (or neurohypophysis) extends anteriorly from the sensory vesicle wall (Figure S1). In ascidians, it contributes to the formation of the adult brain and the associated neural gland [36]. A large mass of mesenchyme cells is present in the posterior ventral part of the trunk, anteriorly to the tail insertion (Figure 1M).

In the posterior dorsal part of the trunk, the endoderm of the pharynx is in contact with the developing ectodermal peribranchial chambers; here, the protostigmata will open during metamorphosis (Figure 2). As is clearly visible in serial histological sections, the two peribranchial chambers are joined dorsally to the nervous system to form a small chamber representing the prospective atrial chamber of the adult (Figure 2D–I). The atrial chamber opens outside through the atrial siphon in the form of a shallow dent in the dorsal trunk (Figures 1L and 2A). However, at this stage, both the siphons are still covered with a thin layer of tunic, preventing circulation of seawater within the larva, which is lecithotrophic and does not filter (Figure 2D). During metamorphosis, the two peribranchial chambers and the atrial chamber will elongate as the pharynx grows, and the stigmata number will increase.

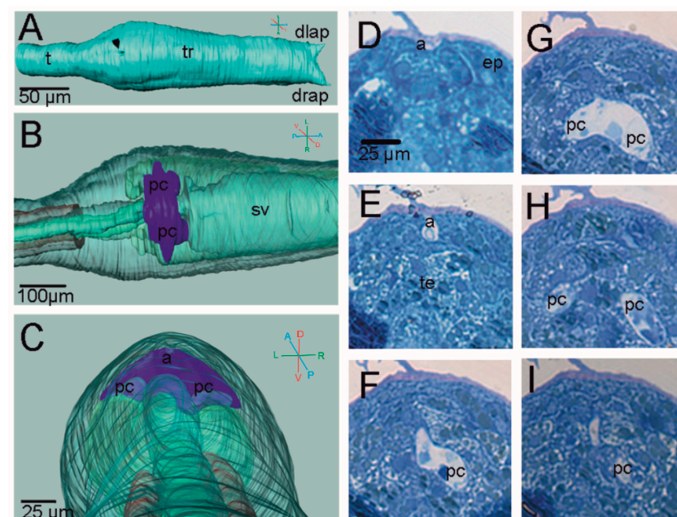


**Figure 2.** Atrial chamber in *H. roretzi*. See Figure 1 for colour code and abbreviations. (A–C) Three-dimensional reconstruction. In B,C the organs are transparent. (A) Dorsal external view showing the dint in correspondence of the atrial siphon (arrowhead). (B) Dorsal view. (C) Frontal-posterior view enlightening the position of the atrial chamber relative to the notochord. (D–I) Serial cross histological sections from anterior to posterior at the level of the atrial and peribranchial chambers. Toluidine blue. The enlargement is the same in (D–I).

The tail, only partially represented in Figure 1, houses the notochord, which is flanked by locomotory musculature on both sides. The notochord extends anteriorly in the trunk

up to the posterior side of the atrial primordium (Figure 1E,F). In the tail, dorsal to the notochord, the neural tube runs up to the posterior end on the larva.

In Figure 3, the 3D reconstructions of three ascidian larvae are compared: *H. roretzi* (solitary, stolidobranch; Figure 3A,B), *Botryllus schlosseri* (colonial, stolidobranch; Figure 3C,D) and *Ciona intestinalis* (solitary, phlebobranch; Figure 3E,F).

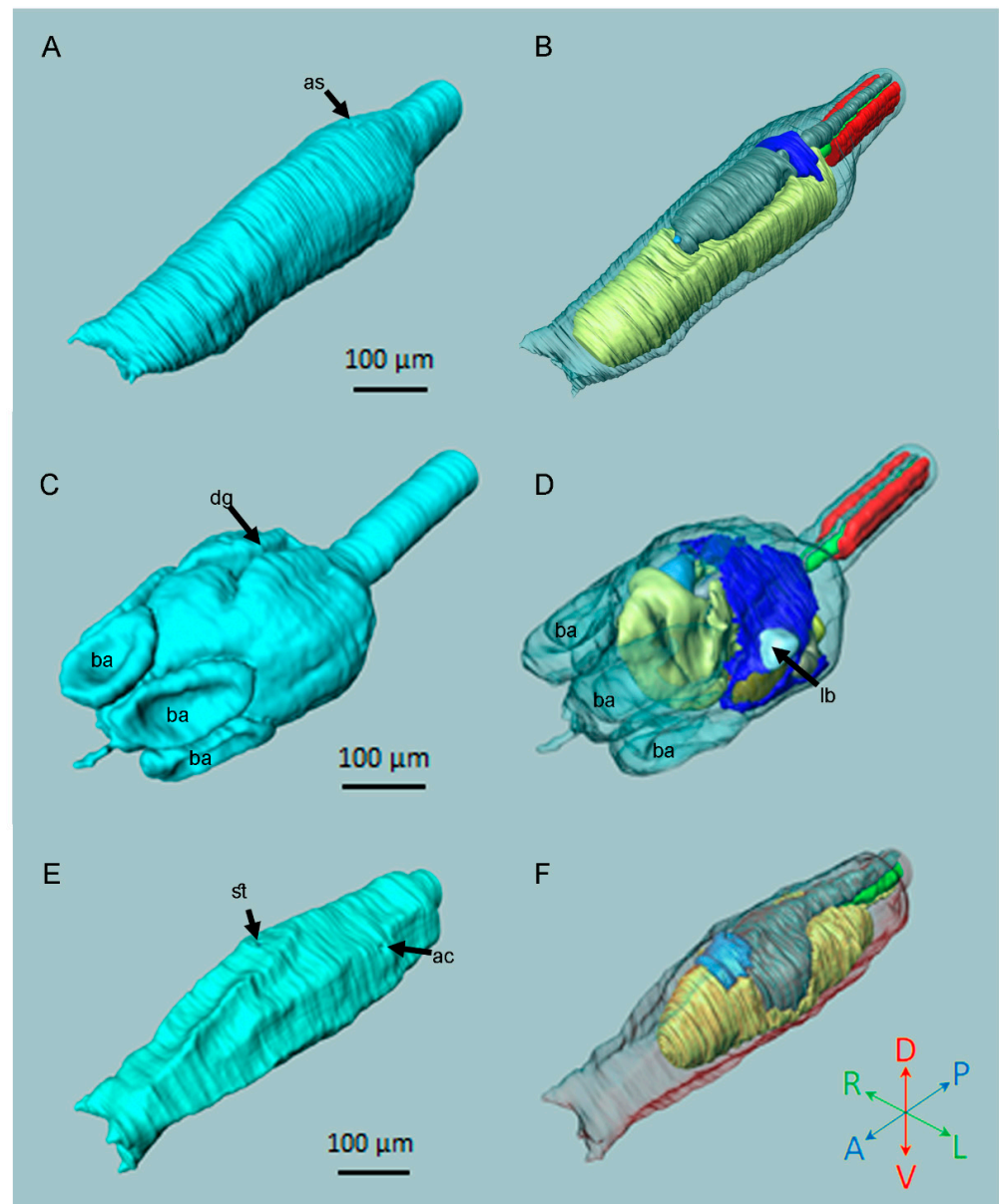


**Figure 3.** Comparison of the 3D reconstructions of three larvae. (A,B) *H. roretzi*. (C,D) *B. schlosseri*. (E,F) *C. intestinalis*. (A,C,E) External views. (B,D,F) Internal views (organs are transparent). Colour code as in Figure 1. Note the different levels of adulthood. ac, left atrial chamber rudiment; as, atrial siphon rudiment; ba, blood ampulla; dg, dorsal groove; lb, left bud; st, stomodeum.

Externally, the trunk of *H. roretzi* (Figure 3A) is more similar to that of the *C. intestinalis* (Figure 3E) as it is elongated, fusiform, and ends at its anterior-most section with three conic papillae. The two stolidobranch species, *H. roretzi* and *B. schlosseri*, share signs of adulthood that are absent in *C. intestinalis* (Figure 3B,D,F; Table 1). In fact, in both stolidobranch species, the atrial chamber forms a well-developed uneven structure; in *C. intestinalis*, the atrial rudiments are in the form of two dorsal-lateral shallow depressions of the epidermis. However, in comparison to *H. roretzi*, *B. schlosseri* shows the highest level

of adulthood, exemplified by the large and perforated pharynx and the differentiated gut (Figure 3D; Table 1). Moreover, the overall morphology of *H. roretzi* is more similar to that of *C. intestinalis*.

**Table 1.** List of anatomical structures represented in the 3D reconstructions of the three selected species. v: present; -: absent.

Organ	<i>H. roretzi</i>	<i>B. schlosseri</i>	<i>C. intestinalis</i>
Atrial chamber	v	v	v
Atrial siphon rudiment	v	v	v
Cerebral ganglion rudiment	-	v	-
Endodermal strand	v	v	v
Epidermis	v	v	v
Esophagus	-	v	-
Heart	-	v	-
Intestine	-	v	-
Left bud rudiment	-	v	-
Neurohypophysial duct	v	v	v
Notochord	v	v	v
Ocellus	v	-	v
Otolith	v	-	v
Oral siphon rudiment	v	v	v
Peribranchial chamber	v	v	-
Pharynx	v	v	v
Photolite	-	v	-
Pyloric caecum and gland	-	v	-
Sensory vesicle	v	v	v
Stomach	-	v	-
Right bud rudiment	-	v	-
Tail musculature	v	v	v

### 3.2. Adhesive Papillae

The swimming larva of *H. roretzi* bears three elongated conic papillae at the anterior tip of the trunk. The papillae lay over the basal lamina and are formed by a monolayer of differentiated ectodermal cells (Figure 4). Below the basal lamina, a conspicuous mesenchymal cell corresponding to each papilla can be consistently recognised (Figure 4B,D,I). In swimming larvae, the papillae are covered by the two layers of tunic (Figure 4A–C).

To determine the relative position and ultrastructural characteristics of the different cell types, we analysed the *H. roretzi* papillae by Transmission Electron Microscopy (TEM) in longitudinal sections. TEM analysis revealed that they are formed by three different cell types that can be identified by their positions and ultrastructural characteristics. The ACCs form the core centre of the papillae; they are elongated cells and bear finger-like protrusions of 2 µm in diameter at their distal ends (Figure 4B). Their nuclei are located close to the basal plasmalemma, and the cytoplasm is rich in vesicles with different electron densities (Figure 4D). Several CCs encircle the ACCs; they have basal nuclei and are easily recognisable by the numerous electron-dense vesicles of different sizes (Figure 4C). Their distal endings bear numerous apical microvilli (Figure 4F). PSNs occupy the lateral part of the papillary body (Figure 4C). They are characterized by a spindle shape, the nuclei being in a central position, and the presence of few small vesicles (Figure 4C,E). Unlike those of the ACCs and CCs, their distal endings do not reach the tip of the papilla, but rather, they stop in a more backward position (Figure 5A).

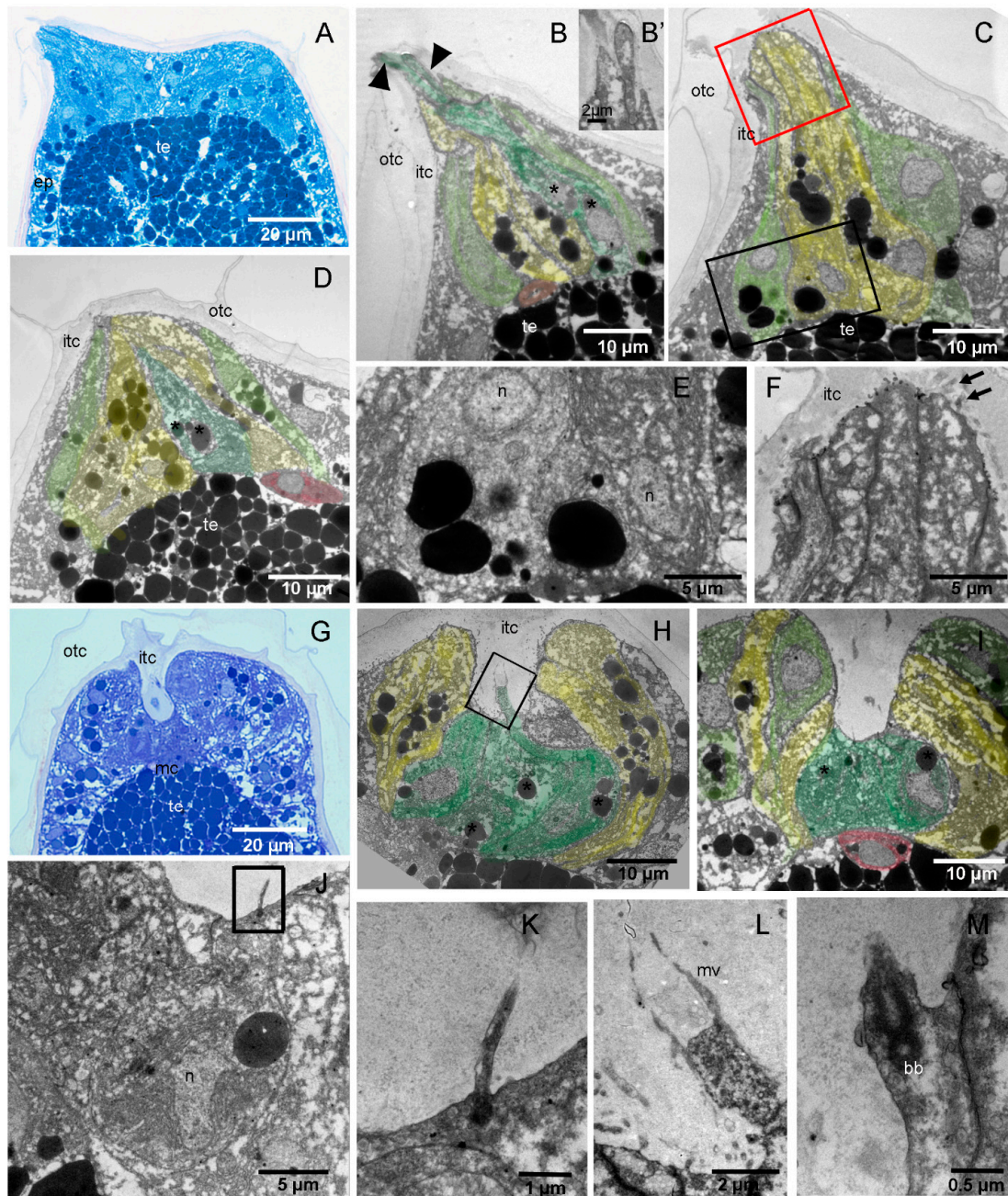


**Figure 4.** Histological and ultrastructural analysis of adhesive papillae in *H. roretzi*. (A–F) Swimming larva: the papillae are conic. (G–M) Adhering larva: the papillae have a central groove. (A,G) Longitudinal sections of the anterior trunk. Toluidine blue. (B–F,H–M) TEM images at different magnifications and different levels of papillae. Colour code: dark green, ACCs; light green, PSNs; red, mesenchyme cells; yellow, CCs. (B–D): Three longitudinal sections of the same papilla. Note that, in (B), the finger-like protrusions (arrowheads) of ACCs are also visible in (B'). The black square area in (C) is enlarged in (E) to show a detail of a PNS basal cytoplasm. The red square area in (C) is enlarged in (F) to show a detail of CCS distal endings with microvilli. Asterisks: vesicles in ACC. (H–I): Two longitudinal sections of the same papilla. The square area in (H) is enlarged in (L) to show ACC apical endings with microvilli, whereas the square area in (J) is enlarged in (K) to show a cilium of PSN. (M): Cilium basal body belonging to a PSN. bb: basal body of a cilium; mc: mesenchymal cell; mv: microvillus; n: nucleus. See also Figure 1 for abbreviations.

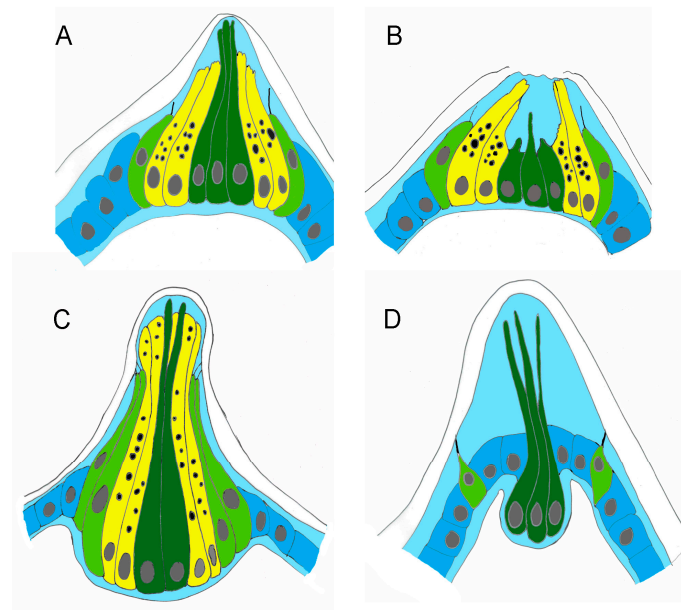


**Figure 5.** Schematic illustrations of adhesive papillae. (A) Swimming larva before metamorphosis of *H. roretzi*. (B) Adhering larva at the onset of metamorphosis of *H. roretzi*. (C) *C. intestinalis* swimming larva (redrawn from Zeng et al., 2019). (D) *B. schlosseri* swimming larva (redrawn from Caicci et al., 2010). Colour code: dark blue, ectodermal cells; dark green, ACCs; light blue, inner compartment of the tunic; light green, PSNs; yellow, CCs.

In adhering larvae, the papillae change shape and form a central groove (Figure 4G). The central ACCs, still recognisable by their finger-like protrusions, are shorter than in swimming larvae and have nuclei with an irregular shape (Figure 4H,I). Their apical endings are located at the base of the groove (Figure 4L). Vesicle-rich CCs form the walls of the groove, and PSNs, exhibiting cilia with atypical morphology, reach the anterior margin of the papilla (Figures 4I,K,M and 5B).

## 4. Discussion

### 4.1. *H. roretzi* Exhibits Minimal Adultation

In this paper, we present the first 3D reconstruction of the larva of *H. roretzi*, an ascidian that has long been established as a model organism in developmental biology studies with more than 400 scientific articles published in the last 10 years (indexed in Scopus). *H. roretzi* is also an important commercial species in Korea and Japan. Since 1995, mass mortality of cultured *H. roretzi*, due to soft tunic syndrome caused by the flagellate *Azumiobodo hoyamushi*, has resulted in significant losses to the ascidian farming industry in Korea [37]. Thus, the detailed knowledge of its biology is an important issue from many points of view. In fact, despite the commercial and scientific importance of this species, the morphology of its larva has been poorly described. In particular, it has been long considered very similar to the well-described larvae of the genera *Ciona* and *Phallusia*, which are phlebobranchi model species [38]. These larvae are simple in their anatomy with no sign of adultation; the pharynx primordium occupies most of the trunk where the mesenchyme is organized in two lateral-ventral pockets [39]. The tail contains 40 notochord cells organized in a central row, flanked by 36 muscle cells on both sides. Dorsally to the notochord, the posterior neural tube is formed by a hollow of ependymal cells [27].

Indeed, it was already known that the larva of *H. roretzi* presents minimal caudalisation, since the tail has 42 rather than the conventional 36 or 38 tail muscle cells [40]. In this species, muscle cells are added to the posterior tip of the tail through the induction of more secondary muscle cells [41]. In this study, we show that the larva also presents minimal adultation as the atrial primordia are recognisable and the atrial siphon already developed, even if a thin layer of tunic occludes its opening. This peculiar condition

has never been described before in the larva of *H. roretzi* but was documented in the larva of *B. schlosseri* [42]. During the embryogenesis of *B. schlosseri*, the atrial chamber originates as a dorsal invagination of the ectoderm, which sinks into the body and bifurcates over the nervous system to form the primordia of the peribranchial chambers. The latter descend ventrally, on both sides, adjacent to the pharyngeal walls. In the contact area, the gill slits perforate and extend to form parallel fissures, the protostigmata. In the phlebobranch *C. intestinalis*, the atrial primordia are paired; they develop as two dorsal, symmetrical invaginations of the ectoderm, one on the left and one on the right, and contact the posterior-most wall of the pharyngeal rudiment. In the mature larva, the two atrial invaginations are opened outward, representing two small chambers, at the bottom of which the protostigmata will perforate [25]. Each atrial chamber forms a rudiment of the atrial siphon that, at the end of metamorphosis, will eventually fuse together and open dorsally to form the unique atrial siphon of the adult. In the juvenile, the two atrial chambers will also converge dorso-medially and fuse with each other, thus creating the unpaired atrial cavity. This important difference in atria formation, together with the gonad location in the lateral body wall, differentiates stolidobranch species from other ascidians.

#### 4.2. The Adhesive Papillae of *H. roretzi* Undergo Dynamic Changes during Adhesion

The papillae of *H. roretzi* were previously described as simple conic ones, similar to those of *C. intestinalis* and *P. mammillata*, even though a detailed description was never reported [27]. Indeed, our TEM analysis revealed that in swimming larvae, the papillae of *H. roretzi* are formed by the same cell types of those of *C. intestinalis*. In particular, the ACCs bear finger-like protrusions and vesicle-rich CCs encircle the ACCs. The PNSs do not reach the papilla apex but are in a more proximal position. This is in accordance with what has been observed in other ascidians species such as *Clavelina lepadiformis* and *Botrylloides leachii* [43,44]. It was proposed that the neuron protrusions reach the substrate and are, therefore, stimulated only once the papillae are attached to the substrate and retracted [44]. Differently from *C. intestinalis*, the hyaline cap, which is formed by the inner tunic compartment on the tip of the papillae, is not recognisable in *H. roretzi*.

Interestingly, our morphological analysis reveals that during settlement, the papillae of *H. roretzi* undergo dynamic changes in shape, assuming a cup-like appearance characterized by a central groove. The ACCs become shorter than in swimming larvae and have nuclei with irregular shapes, suggesting that they undergo a deep rearrangement. Overall, the papillae are less extended and the PNSs now reach the anterior endings in a position where they can contact the substrate. We hypothesize that some cell components are also degenerating. These observations, which recall those reported for species with “scyphate papillae with axial protrusions” [27], suggest that the adhesive organs of *H. roretzi* are more complex than previously supposed and deserve to be further analysed also with a molecular approach.

**Supplementary Materials:** The following are available online at <https://www.mdpi.com/article/10.3390/jmse10010011/s1>, Figure S1: Interactive PDF file of *H. roretzi* 3D reconstruction. Table S1: measurements of trunk length and width of *H. roretzi* larvae; Video S1: video of *H. roretzi* 3D reconstruction.

**Author Contributions:** Conceptualization, L.M. and R.P.; 3D reconstruction, F.C.; histology and TEM, L.M. and F.C.; morphometric analysis, S.M.; result interpretation and discussion, L.M., F.C., C.A., V.V., S.M. and R.P.; writing, R.P. and L.M. All authors have read and agreed to the published version of the manuscript.

**Funding:** This research received no external funding.

**Institutional Review Board Statement:** Not applicable for studies on tunicates.

**Informed Consent Statement:** Not applicable.

**Acknowledgments:** The authors thank Paolo Burighel for his helpful discussions, Hiroki Nishida for specimen collection assistance, Karla Palmieri for English revision and Emmanuel Faure for hosting the 3D model on MorphoNet.org.

**Conflicts of Interest:** The authors declare no conflict of interest.

### Abbreviations

List of abbreviations present in the text.

a	atrium
ac	left atrial chamber rudiment
ACC	axial columnar cell
as	atrial siphon rudiment
ba	blood ampulla
bb	basal body of a cilium
CC	collocyte
dlap	dorsal left adhesive papilla
drap	dorsal right adhesive papilla
dg	dorsal groove
ep	epidermis
es	endodermal strand
itc	inner tunic compartment
lb	left bud
m	muscle
mc	mesenchymal cell
me	mesenchyme
mv	microvillus
n	nucleus
nc	notochord
ne	neck
oc	ocellus
ot	otolith
otc	outer tunic compartment
pc	peribranchial chambers
PSN	primary sensory neuron
te	trunk endoderm
tf	tail fin
st	stomodeum
sv	sensory vesicle
vap	ventral adhesive papilla
vg	visceral ganglion

### References

1. Delsuc, F.; Brinkmann, H.; Chourrout, D.; Philippe, H. Tunicates and not cephalochordates are the closest living relatives of vertebrates. *Nature* **2006**, *439*, 965–968. [[CrossRef](#)]
2. Sepúlveda, R.; Rozbaczylo, N.; Ibáñez, C.; Flores, M.; Cancino, J. Ascidian-associated polychaetes: Ecological implications of aggregation size and tube-building chaetopterids on assemblage structure in the Southeastern Pacific Ocean. *Mar. Biodivers* **2014**, *45*, 733–741. [[CrossRef](#)]
3. Voultziadou, E.; Kyrodinou, M.; Antoniadou, C.; Vafidis, D. Sponge epibionts on ecosystem-engineering ascidians: The case of *Microcosmus sabatieri*. *Estuar. Coast. Shelf Sci.* **2010**, *86*, 598–606. [[CrossRef](#)]
4. Mercurio, S.; Messinetti, S.; Manenti, R.; Ficaretola, G.F.; Pennati, R. Embryotoxicity characterization of the flame retardant tris(1-chloro-2-propyl)phosphate (TCPP) in the invertebrate chordate *Ciona intestinalis*. *J. Exp. Zool. Part A Ecol. Integr. Physiol.* **2021**, *335*, 339–347. [[CrossRef](#)] [[PubMed](#)]
5. Messinetti, S.; Mercurio, S.; Pennati, R. Effects of bisphenol A on the development of pigmented organs in the ascidian *Phallusia mammillata*. *Invertebr. Biol.* **2018**, *137*, 329–338. [[CrossRef](#)]
6. Messinetti, S.; Mercurio, S.; Pennati, R. Bisphenol A affects neural development of the ascidian *Ciona robusta*. *J. Exp. Zool. Part A Ecol. Integr. Physiol.* **2019**, *331*, 5–16. [[CrossRef](#)]
7. Lambert, G.; Karney, R.C.; Rhee, W.Y.; Carman, M. Wild and cultured edible tunicates: A review. *Manag. Biol. Invasions* **2016**, *7*, 59–66. [[CrossRef](#)]
8. Coleman, F.C.; Williams, S.L. Overexploiting marine ecosystem engineers: Potential consequences for biodiversity. *Trends Ecol. Evol.* **2002**, *17*, 40–44. [[CrossRef](#)]

9. Wang, K.; Dantec, C.; Lemaire, P.; Onuma, T.A.; Nishida, H. Genome-wide survey of miRNAs and their evolutionary history in the ascidian, *Halocynthia roretzi*. *BMC Genom.* **2017**, *18*, 314. [[CrossRef](#)]
10. Brozovic, M.; Martin, C.; Dantec, C.; Dauga, D.; Mendez, M.; Simion, P.; Percher, M.; Laporte, B.; Scornavacca, C.; Di Gregorio, A.; et al. ANISEED 2015: A digital framework for the comparative developmental biology of ascidians. *Nucleic Acids Res.* **2016**, *44*, D808–D818. [[CrossRef](#)]
11. Lambert, G. Invasive sea squirts: A growing global problem. *J. Exp. Mar. Biol. Ecol.* **2007**, *342*, 3–4. [[CrossRef](#)]
12. Brown, F.D.; Swalla, B.J. Evolution and development of budding by stem cells: Ascidian coloniality as a case study. *Dev. Biol.* **2012**, *369*, 151–162. [[CrossRef](#)] [[PubMed](#)]
13. Alié, A.; Hiebert, L.S.; Scelzo, M.; Tiozzo, S. The eventful history of nonembryonic development in tunicates. *J. Exp. Zool. B Mol. Dev. Evol.* **2021**, *336*, 250–266. [[CrossRef](#)] [[PubMed](#)]
14. Berrill, N.J.; Watson, D.M.S.; II-Studies in Tunicate development. Part V-The evolution and classification of Ascidians. *Philos. Trans. R. Soc. Lond. B Biol. Sci.* **1936**, *226*, 43–70. [[CrossRef](#)]
15. Rubinstein, N.D.; Feldstein, T.; Shenkar, N.; Botero-Castro, F.; Griggio, F.; Mastrototaro, F.; Delsuc, F.; Douzery, E.J.P.; Gissi, C.; Huchon, D. Deep Sequencing of Mixed Total DNA without Barcodes Allows Efficient Assembly of Highly Plastic Ascidian Mitochondrial Genomes. *Genome Biol. Evol.* **2013**, *5*, 1185–1199. [[CrossRef](#)]
16. Tsagkogeorga, G.; Turon, X.; Hopcroft, R.R.; Tilak, M.-K.; Feldstein, T.; Shenkar, N.; Loya, Y.; Huchon, D.; Douzery, E.J.P.; Delsuc, F. An updated 18S rRNA phylogeny of tunicates based on mixture and secondary structure models. *BMC Evol. Biol.* **2009**, *9*, 187. [[CrossRef](#)]
17. DeBiasse, M.B.; Colgan, W.N.; Harris, L.; Davidson, B.; Ryan, J.F. Inferring Tunicate Relationships and the Evolution of the Tunicate Hox Cluster with the Genome of *Corella inflata*. *Genome Biol. Evol.* **2020**, *12*, 948–964. [[CrossRef](#)]
18. Lübbering, B.; Goffinet, G. Ultrastructural survey of tunic morphogenesis in the larval and young adult ascidian *Asciidiella aspersa* (Tunicata, Ascidiacea). *Belg. J. Zool.* **1991**, *121*, 39–53.
19. Cloney, R.A.; Cavey, M.J. Ascidian larval tunic: Extraembryonic structures influence morphogenesis. *Cell Tissue Res.* **1982**, *222*, 547–562. [[CrossRef](#)]
20. Cavey, M.J.; Cloney, R.A. Development of the larval tunic in a compound ascidian: Morphogenetic events in the embryos of *Distaplia occidentalis*. *Can. J. Zool.* **1984**, *62*, 2392–2400. [[CrossRef](#)]
21. Hotta, K.; Dauga, D.; Manni, L. The ontology of the anatomy and development of the solitary ascidian *Ciona*: The swimming larva and its metamorphosis. *Sci. Rep.* **2020**, *10*, 17916. [[CrossRef](#)]
22. Jeffery, W.R.; Swalla, B.J. Evolution of alternate modes of development in ascidians. *BioEssays* **1992**, *14*, 219–226. [[CrossRef](#)] [[PubMed](#)]
23. Zaniolo, G.; Manni, L.; Burighel, P. Ovulation and embryo-parent relationships in *Botrylloides leachi* (Ascidiacea, Tunicata). *Invertebr. Reprod. Dev.* **1994**, *25*, 215–225. [[CrossRef](#)]
24. Zaniolo, G.; Manni, L.; Brunetti, R.; Burighel, P. Brood pouch differentiation in *Botrylloides violaceus*, a viviparous ascidian (Tunicata). *Invertebr. Reprod. Dev.* **1998**, *33*, 11–23. [[CrossRef](#)]
25. Manni, L.; Lane, N.J.; Joly, J.-S.; Gasparini, F.; Tiozzo, S.; Caicci, F.; Zaniolo, G.; Burighel, P. Neurogenic and non-neurogenic placodes in ascidians. *J. Exp. Zool. B Mol. Dev. Evol.* **2004**, *302*, 483–504. [[CrossRef](#)]
26. Kowarsky, M.; Anselmi, C.; Hotta, K.; Burighel, P.; Zaniolo, G.; Caicci, F.; Rosental, B.; Neff, N.F.; Ishizuka, K.J.; Palmeri, K.J.; et al. Sexual and asexual development: Two distinct programs producing the same tunicate. *Cell Rep.* **2021**, *34*, 108681. [[CrossRef](#)]
27. Burighel, P.; Cloney, R.A. Urochordata: Ascidiacea. In *Microscopic Anatomy of Invertebrates*, Vol 15. *Hemichordata, Chaetognatha, and the Invertebrate Chordates*; Harrison, F.W., Rupert, E.E., Eds.; Wiley-Liss, Inc.: New York, NY, USA, 1997; Volume 15.
28. Dolcemascolo, G.; Pennati, R.; De Bernardi, F.; Damiani, F.; Gianguzza, M. Ultrastructural comparative analysis on the adhesive papillae of the swimming larvae of three ascidian species. *Invertebr. Surviv. J.* **2009**, *6*, S77–S86.
29. Caicci, F.; Zaniolo, G.; Burighel, P.; Degasperi, V.; Gasparini, F.; Manni, L. Differentiation of papillae and rostral sensory neurons in the larva of the ascidian *Botryllus schlosseri* (Tunicata). *J. Comp. Neurol.* **2010**, *518*, 547–566. [[CrossRef](#)]
30. Pennati, R.; Ficetola, G.F.; Brunetti, R.; Caicci, F.; Gasparini, F.; Griggio, F.; Sato, A.; Stach, T.; Kaul-Strehlow, S.; Gissi, C.; et al. Morphological Differences between Larvae of the *Ciona intestinalis* Species Complex: Hints for a Valid Taxonomic Definition of Distinct Species. *PLoS ONE* **2015**, *10*, e0122879. [[CrossRef](#)]
31. Brunetti, R.; Gissi, C.; Pennati, R.; Caicci, F.; Gasparini, F.; Manni, L. Morphological evidence that the molecularly determined *Ciona intestinalis* type A and type B are different species: *Ciona robusta* and *Ciona intestinalis*. *J. Zool. Syst. Evol. Res.* **2015**, *53*, 186–193. [[CrossRef](#)]
32. Zeng, F.; Wunderer, J.; Salvenmoser, W.; Ederth, T.; Rothbacher, U. Identifying adhesive components in a model tunicate. *Philos. Trans. R. Soc. B Biol. Sci.* **2019**, *374*, 20190197. [[CrossRef](#)]
33. Horie, T.; Kusakabe, T.; Tsuda, M. Glutamatergic networks in the *Ciona intestinalis* larva. *J. Comp. Neurol.* **2008**, *508*, 249–263. [[CrossRef](#)] [[PubMed](#)]
34. Leggio, B.; Laussu, J.; Carlier, A.; Godin, C.; Lemaire, P.; Faure, E. MorphoNet: An interactive online morphological browser to explore complex multi-scale data. *Nat. Commun.* **2019**, *10*, 2812. [[CrossRef](#)] [[PubMed](#)]
35. Manni, L.; Pennati, R. Tunicata. In *Structure and Evolution of Invertebrate Nervous Systems*; Schmidt-Rhaesa, G.P.A., Harzsch, S., Eds.; Oxford University Press: Oxford, UK, 2016. [[CrossRef](#)]

36. Manni, L.; Agnoletto, A.; Zaniolo, G.; Burighel, P. Stomodeal and neurohypophysial placodes in *Ciona intestinalis*: Insights into the origin of the pituitary gland. *J. Exp. Zool. Part B Mol. Dev. Evol.* **2005**, *304*, 324–339. [[CrossRef](#)]
37. Kumagai, A.; Ito, H.; Sasaki, R. Detection of the kinetoplastid *Azumiobodo hoyamushi*, the causative agent of soft tunic syndrome, in wild ascidians *Halocynthia roretzi*. *Dis. Aquat. Organ.* **2013**, *106*, 267–271. [[CrossRef](#)] [[PubMed](#)]
38. Hudson, C.; Yasuo, H. Similarity and diversity in mechanisms of muscle fate induction between ascidian species. *Biol. Cell.* **2008**, *100*, 265–277. [[CrossRef](#)] [[PubMed](#)]
39. Katz, M.J. Comparative anatomy of the tunicate tadpole, *Ciona intestinalis*. *Biol. Bull.* **1983**, *164*, 1–27. [[CrossRef](#)]
40. Passamaneck, Y.J.; Di Gregorio, A. *Ciona intestinalis*: Chordate development made simple. *Dev. Dyn.* **2005**, *233*, 1–19. [[CrossRef](#)] [[PubMed](#)]
41. Nishida, H. Determinative mechanisms in secondary muscle lineages of ascidian embryos: Development of muscle-specific features in isolated muscle progenitor cells. *Development* **1990**, *108*, 559–568. [[CrossRef](#)] [[PubMed](#)]
42. Manni, L.; Lane, N.J.; Zaniolo, G.; Burighel, P. Cell reorganisation during epithelial fusion and perforation: The case of ascidian branchial fissures. *Dev. Dyn.* **2002**, *224*, 303–313. [[CrossRef](#)]
43. Pennati, R.; Zega, G.; Groppelli, S.; De Bernardi, F. Immunohistochemical analysis of the adhesive papillae of *Botrylloides leachi* (Chordata, Tunicata, Ascidiacea): Implications for their sensory function. *Ital. J. Zool.* **2007**, *74*, 325–329. [[CrossRef](#)]
44. Pennati, R.; Groppelli, S.; De Bernardi, F.; Mastrototaro, F.; Zega, G. Immunohistochemical analysis of adhesive papillae of *Clavelina lepadiformis* (Müller, 1776) and *Clavelina phlegraea* (Salfi, 1929) (Tunicata, Ascidiacea). *Eur. J. Histochem.* **2009**, *53*, e4. [[CrossRef](#)] [[PubMed](#)]